Expanded View Figures

Figure EV1. The centrosomes in qNSCs are immature.

A Larval brains at 2 h after larval hatching (ALH) from *grainy head* (*grh)*-Gal4; UAS-CD8-GFP were labeled with Asterless, Deadpan (Dpn) and GFP. Arrows indicate the centrosomes.

B Larval brains at 0 h ALH from *grh*-Gal4; UAS-CD8-GFP were labeled with CNN, Asl, Deadpan (Dpn), and GFP. Arrows indicate the centrosomes.

C Wild-type larval brains expressing CNN-GFP (MiMIC line; BDSC#60266) at 0 h ALH were labeled with GFP, Dpn, and Msps. A representative qNSC and interphase Mushroom body (MB) NSC are shown.

D Wild-type larval brains expressing *grh*>CD8-GFP at 6 h ALH were labeled with CNN, Asl, Dpn, and GFP. Arrows indicate the centrosomes.

E Quantification of the cell diameter of CNN-negative vs CNN-positive qNSCs from wild-type brains expressing *grh*>CD8-GFP at 6 h ALH. $n = 26$ NSCs for CNN-negative qNSCs; $n = 14$ NSCs for CNN-positive qNSCs. ****$P < 0.0001$.

F Quantification graph of the ratio of CNN intensity between qNSCs and mushroom body (MB) NSCs from 0 h ALH and 6 h ALH larval brains in (B, D). $n = 40$ NSCs for 0 h ALH; $n = 99$ for 6 h ALH. ****$P < 0.0001$.

G Wild-type larval brains expressing *grh*>CD8-GFP at 0 h ALH were stained with γ-tubulin, Dpn, and GFP. A representative qNSC and interphase Mushroom body (MB) NSC are shown. Arrows indicate the centrosome.

H Wild-type larval brains expressing *grh*>CD8-GFP at 0 h ALH and 6 h ALH were labeled with γ-tubulin, Dpn, and GFP. Arrows indicate the centrosome.

I Quantification graph of the ratio of γ-tub intensity between qNSCs and mushroom body (MB) NSCs from 0 h ALH and 6 h ALH larval brains in (H). $n = 84$ NSCs for 0 h ALH; $n = 63$ NSCs for 6 h ALH. ****$P < 0.0001$.

J Larval brains at 0 h ALH from *insc*-Gal4; UAS-β-tubulin-Venus were labeled with GFP, Msps and Dpn. Quiescent NSCs at the CB are shown. The arrow points at the centrosome.

K Wild-type larval brains expressing *grh*>CD8-GFP at 6 h ALH were labeled with α-tubulin, Dpn and GFP, and wild-type larval brains at 16 h ALH were labeled with α-tubulin, Msps and Dpn.

L Larval brains expressing Msps-GFP under the control of *insc*-Gal4 at 16 h ALH were labeled with GFP, Dpn, and Mira.

Data information: In (E, F, I), data are presented as mean ± SD. In (E, F, I), statistical significances were determined by two-tailed Student's *t*-test. Scale bars: 10 μm.

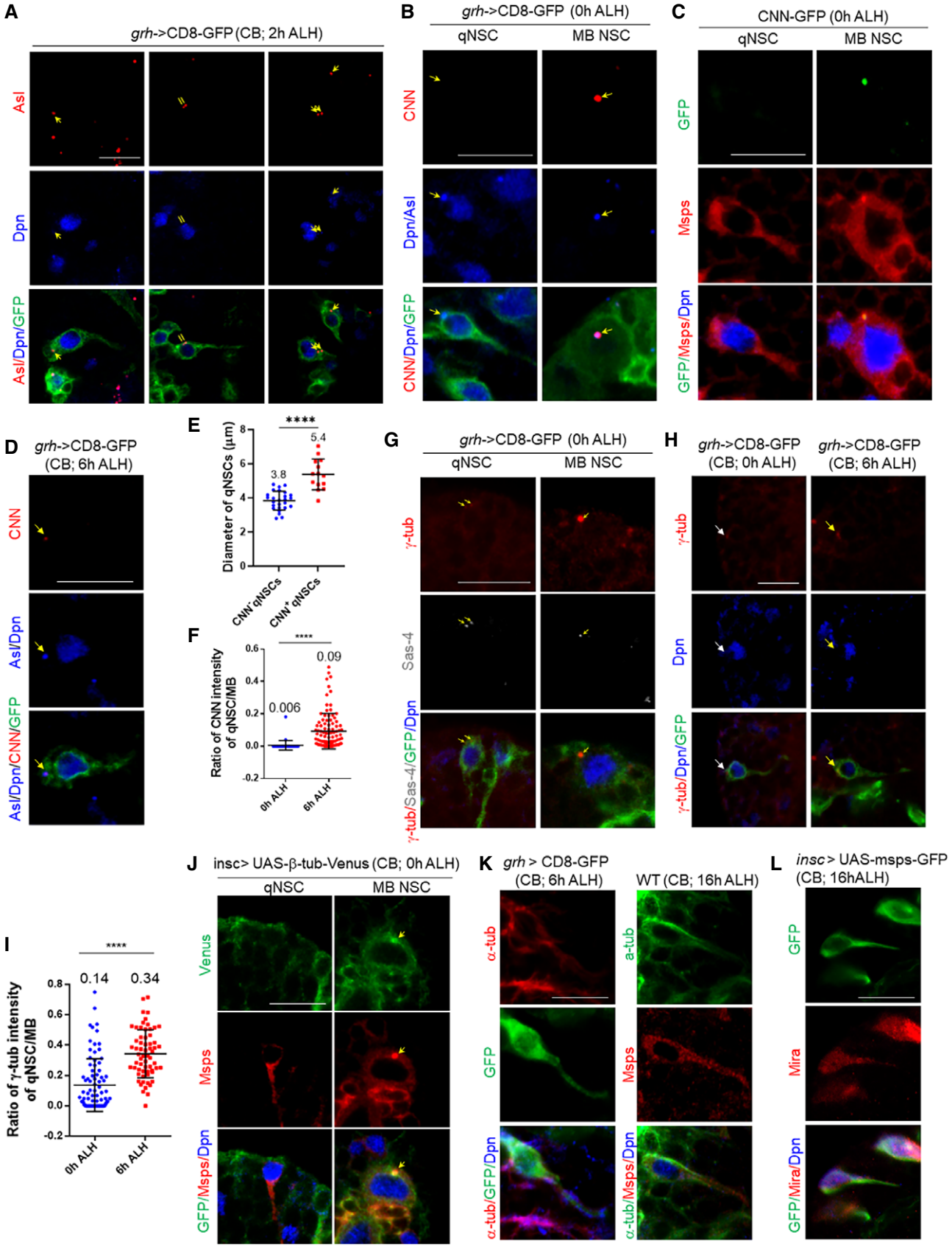

Figure EV1.

Figure EV2. Msps, but not Arl2, is essential for NSC reactivation.

A Larval brains at 24 h ALH from control (*insc*-Gal4; *UAS-dicer2* / *UAS-β-Gal* RNAi), *arl2* RNAi (VDRC#110627); *UAS-dicer2* and *UAS-arl2^{T30N}* under the control of *insc*-Gal4 were analyzed for EdU incorporation. NSCs were marked by Dpn and Mira. Arrows indicate EdU- negative NSCs.

B Quantification of EdU-negative NSCs per brain lobe for genotypes in (A). $n = 15$ BL for control; $n = 11$ BL for *arl2* RNAi; $n = 11$ BL for *UAS-arl2^{T30N}*. ****$P < 0.0001$; $P = 0.1547$ (ns).

C Larval brains from various genotypes were labeled with Msps, Dpn, and GFP at the indicated time points. Left panels, wild-type, *msps^{924}*, and *msps^{P18}*, all expressing CD8-GFP under the control of *grh*-Gal4. Middle panels, control (*UAS-β-Gal* RNAi) and *msps* RNAi expressing CD8-GFP under the control of *insc*-Gal4. Right panels, control (*UAS-β-Gal* RNAi) and *msps* RNAi under *grh*-Gal4. Note that not all qNSCs were labeled by *grh*>CD8-GFP at early larval stages. White arrows point at the cell body and yellow arrows indicate the primary protrusion of the qNSC.

D Larval brains at 0 h ALH from wild-type, *msps^{924}*, and *msps^{P18}* expressing *grh*>CD8-GFP were labeled with Msps, Dpn, and GFP.

E Larval brains at 24 h ALH from control (*grh*>CD8-GFP) and *msps^{924}* expressing *grh*>CD8-GFP were labeled with Dpn and GFP. Single NSC lineage in the box was magnified in the panel on the right. Arrows indicate NSCs.

F Quantification of the total NSC number from genotypes in (E). $n = 10$ BL for control; $n = 14$ BL for *msps^{924}*. ****$P < 0.0001$.

Data information: in (B, E), data are presented as mean ± SD. In (B), statistical significance was determined by one-way ANOVA with multiple comparisons. In (E), statistical significance was determined by two-tailed Student's *t*-test. Scale bars: 10 μm.

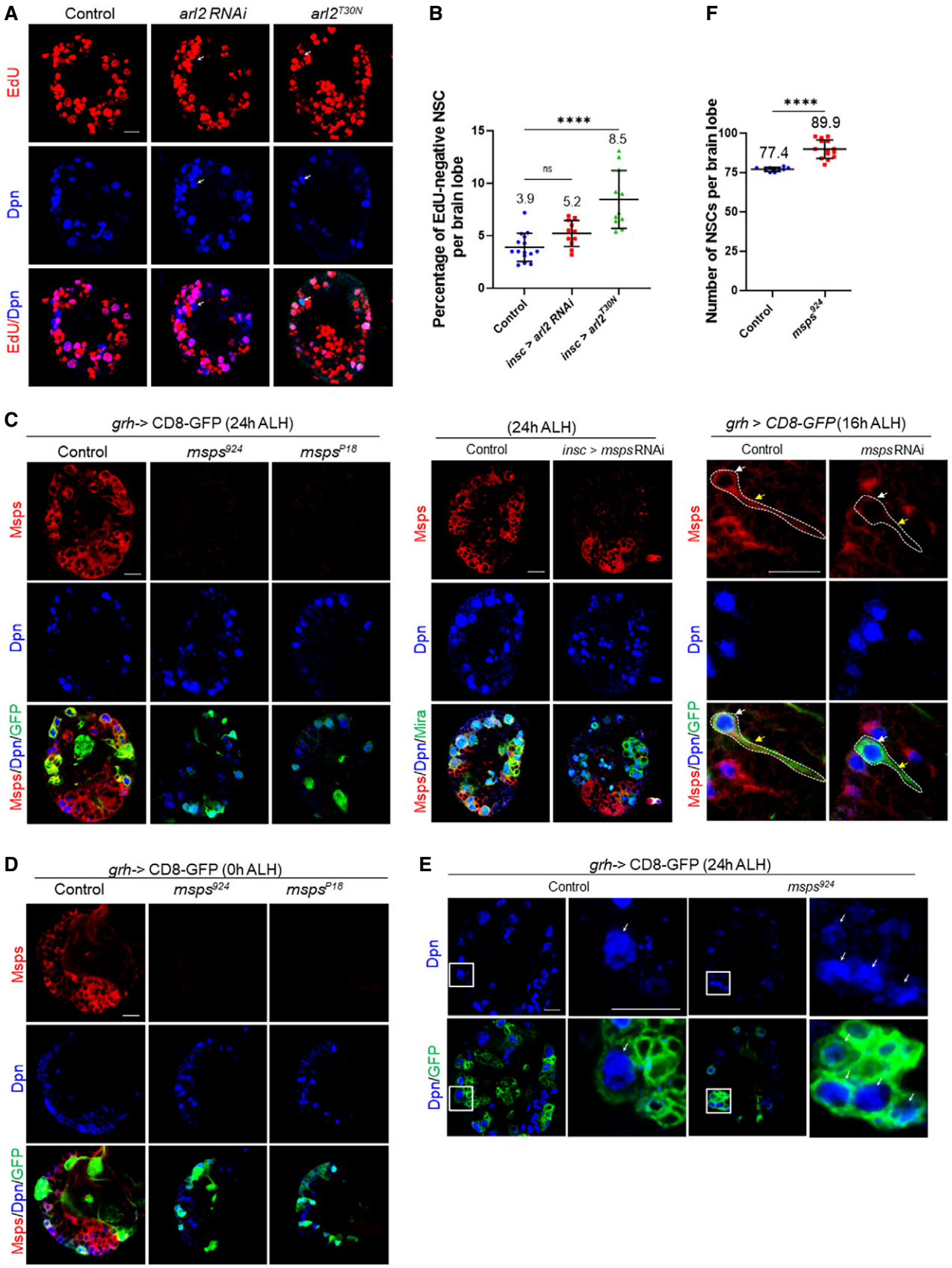

Figure EV2.

Figure EV3. Microtubule assembly in the primary protrusion of qNSCs is centrosome-independent.

A, B (A) Larval brains at 6 h ALH from *sas-4* RNAi with *grh*-Gal4; *UAS-EB1-GFP* were stained with Sas-4, Dpn, and GFP. Primary protrusion of qNSCs was marked by GFP. (B) Larval brains at 6 h ALH *ana2* RNAi *ana2*^{719}/+ with *grh*-Gal4; *UAS-EB1-GFP* were stained with Ana2, Dpn, and GFP. Primary protrusion of qNSCs was marked by GFP. Efficient knockdown of *sas4* or *ana2* in GFP-positive qNSCs with primary protrusion is shown in (A, B). Sas4 and Ana2 staining were present in some of the GFP-negative NSCs, which were shown as positive controls in (A, B). Arrows indicate the centrosome.

C Kymograph of EB-GFP comet movement in the primary protrusion of qNSCs from control (*UAS-β-Gal* RNAi), *sas-4* RNAi (VDRC#106051), and *ana2* RNAi; *ana2*^{719}/+ with *grh*-Gal4; *UAS-EB1-GFP* at 6 h ALH. The horizontal arrow indicates anterograde movement direction from the cell body to the tip of the primary protrusion in qNSCs. Kymographs with and without colored lines were shown.

D Quantification graph of the fold change of the number of EB1-GFP comets in the primary protrusion of qNSCs from genotypes in (C). $n = 2$ individual experiments per genotype. Control vs *sas-4* RNAi, $P = 0.6174$ (ns); control vs *ana2* RNAi; *ana2*^{719}/+, $P = 0.9941$ (ns).

E Larval brains at 24 h ALH from control (*grh*-Gal4; *UAS-dicer2*/*UAS-β-Gal* RNAi) and *sas-4* RNAi (VDRC#106051) and *ana2* RNAi; *ana2*^{719}/+ controlled under *grh*-Gal4 were analyzed for EdU incorporation. NSCs were marked by Dpn and Mira. Arrows point at EdU-negative NSCs.

F Quantification graph of EdU-negative NSCs per brain lobe for genotypes in (E). ****$P < 0.0001$; $P = 0.9106$ (ns). Control, 6.0%, $n = 14$ BL; *sas-4* RNAi, 12.6%, $n = 18$ BL. *ana2* RNAi, *ana2*^{719}/+, 5.6%, $n = 14$ BL.

G Quantification graph of the percentage of qNSCs with primary protrusion per brain lobe for genotypes in (E). Control, 4.9%, $n = 9$; *sas-4* RNAi, 10.7%, $n = 14$ BL; *ana2* RNAi, *ana2*^{719}/+, 4.7%, $n = 11$ BL. ****$P < 0.0001$; $P = 0.8681$ (ns).

H Larval brains at 24 h ALH from control and *msps*^{924} expressing *grh*>CD8-GFP were labeled with Asl, Dpn, and GFP. Arrows indicate the centrosome.

I Quantification graph of the percentage of qNSCs with Asl localized to apical, lateral, and PIS region of the qNSCs for the genotypes in (H). $n = 10$ NSCs for control; $n = 10$ NSCs for *sas-4* RNAi; $n = 16$ NSCs for *ana2* RNAi, *ana2*^{719}/+.

J Larval brains at 24 h ALH from control (*insc*-Gal4; *UAS-dicer2*/*UAS-β-Gal* RNAi) and γ-*tub23C* RNAi I (BDSC#42799) and γ-*tub23C* RNAi II (BDSC#31204) controlled under *insc*-Gal4 were analyzed for EdU incorporation. NSCs were marked by Dpn and Mira.

K Quantification graph of EdU-negative NSCs per brain lobe for genotypes in (J). $n = 12$ BL for control; $n = 11$ BL for γ-*tub23C* RNAi I; $n = 14$ BL for γ-*tub23C* RNAi II. Control vs γ-*tub23C* RNAi I, $P = 0.8825$ (ns); control vs γ-*tub23C* RNAi II, $P = 0.8379$ (ns).

L Larval brains at 24 h ALH for genotypes in (J) were stained with γ-tub, Msps, and Dpn. Arrows indicate the centrosome.

Data information: in (D, F, G, I, K), data are presented as mean ± SD. In (D, F, G, K), statistical significance was determined by one-way ANOVA with multiple comparisons. In (I), statistical significance was determined by two-way ANOVA with multiple comparisons. Scale bars: 10 μm.

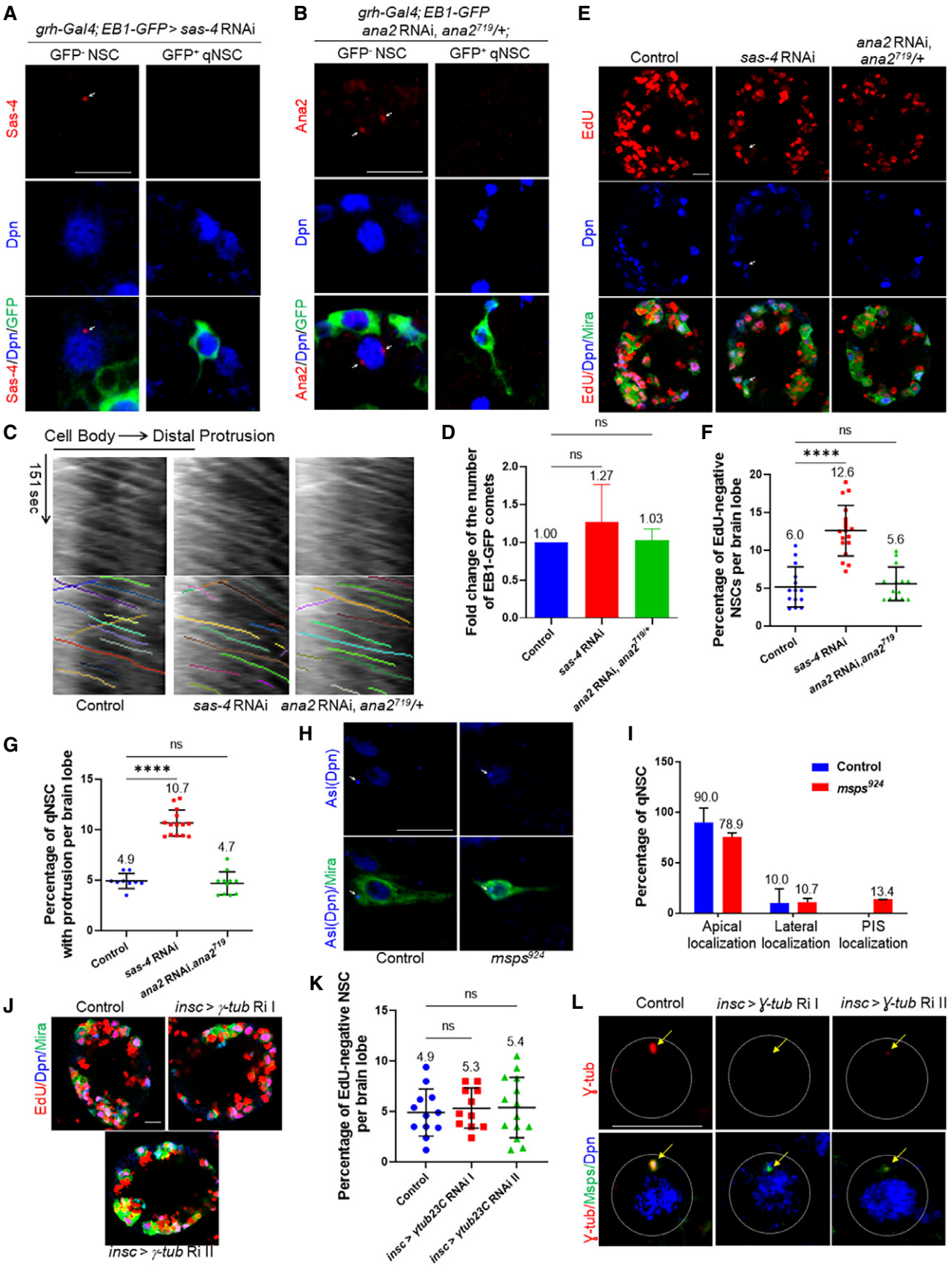

Figure EV3.

Figure EV4. E-cad delocalization in *msps*-depleted qNSCs.

A Larval brains at 24 h ALH from control (*grh*>CD8-GFP) and $msps^{924}$ expressing *grh*>CD8-GFP were analyzed for α-tubulin (α-tub), and NSCs were labeled with Dpn and GFP. Boxes indicate the area that α-tub intensity was measured.

B Quantification graph of the α-tub intensity for the genotypes in (A). $n = 39$ NSC for control; $n = 37$ NSC for $msps^{924}$. Two biological replicates per each genotype. $P = 0.1000$.

C Larval VNCs at 16 h ALH from the control (*grh*-Gal4 *UAS-CD8-GFP*; *UAS-Dicer2* / *UAS-β-Gal RNAi*) and *msps* RNAi under the control of with *grh*-Gal4 *UAS-CD8-GFP*; *UAS-Dicer2* were labeled with E-cadherin, Dpn, and GFP. NSC-neuropil contact was marked by dashed lines, and NSC-neuropil contact points were circled.

D Quantification of E-cadherin basal localization at NSC-neuropil contact sites in qNSCs from genotypes in (C). "No E-cad" means absent or strongly reduced E-cad observed at the tip of the protrusion in qNSCs. $n = 39$ NSC for control; $n = 44$ NSC for *msps* RNAi. Two biological replicates per genotype. ***$P = 0.0008$.

E Larval brains at 24 h ALH from mutant control (*grh*-Gal4; *UAS-β-Gal* RNAi; $klp64D^{k5h}$) and rescued animals (*grh*-Gal4; *UAS-klp64D*; $klp64D^{k5h}$) were analyzed for EdU incorporation. NSCs were labeled with EdU, Dpn, and Mira. The number of EdU-negative NSCs was reduced to 10.5% in rescued animals ($n = 11$ BL), which was significantly lower than 25.2% in $klp64D^{k5h}$ ($n = 13$ BL), and indistinguishable from the wild-type control (11.4%, $n = 13$ BL). EdU-negative NSCs are indicated by arrows.

F Quantification graph displaying NSCs remaining primary protrusion per brain lobe for genotypes in (E). ****$P < 0.0001$; $P = 0.7542$ (ns). Only 6.1% of ($n = 14$ BL) NSC remained cellular protrusion in the rescued animals, which was significantly reduced in contrast to 14.5% in $klp64D^{k5h}$ ($n = 10$ BL), and similar to the wild-type control (5.3%, $n = 10$ BL).

G Quantification graph showing NSCs negative for EdU incorporation for genotypes in (E). $n = 13$ BL for control; $n = 13$ BL for $klp64D^{k5h}$; $n = 11$ BL for *UAS-klp64D*; $klp64D^{k5h}$. ****$P < 0.0001$; $P = 0.9346$ (ns).

H Quantification graph depicting NSCs positive for PH3 for genotypes in (E). ****$P < 0.0001$; $P = 0.8768$ (ns). The number of PH3-positive mitotic NSCs in rescued animals (19.7%, $n = 14$ BL) were increased compared with $klp64D^{k5h}$ (9.9%, $n = 11$ BL). Wild-type control, 20.7%, $n = 10$ BL.

I Larval brains at 24 h ALH from wild-type and hemizygous animals $klp64D^{Df/+}$ (Df(3L)BSC371; BDSC# 24395) were examined for EdU incorporation. NSCs were labeled with EdU and Dpn. Only 7.3% of ($n = 16$ BL) hemizygous $klp64D^{Df/+}$ NSCs did not incorporate EdU, which was indistinguishable from 8.4% in wild-type control ($n = 15$ BL).

J Quantification graph showing the percentage of EdU-negative NSCs per brain lobe for genotypes in (I). $n = 15$ BL for control; $n = 16$ BL for $klp64D^{Df/+}$. $P = 0.2042$ (ns).

K Larval brains at 24 h ALH from control (*insc*-Gal4, *tub*-$Gal80^{ts}$/*UAS-β-Gal* RNAi;) and *msps* RNAi driven by *insc*-Gal4, *tub*-$Gal80^{ts}$ were analyzed for EdU incorporation. NSCs were labeled with EdU, Dpn, and Mira. EdU-negative NSCs are indicated by arrows.

L Quantification graph displaying the percentage of NSCs that fail to incorporate EdU per brain lobe for genotypes in (K). $n = 13$ BL for control; $n = 15$ BL for *msps* RNAi. ****$P < 0.0001$.

M Larval brains at 16 h ALH from *grh*-Gal4>UASp-E-cad-GFP were analyzed for GFP and E-cad. NSCs were labeled by Dpn. E-cad at the protrusion tip is circled. The cell body of qNSCs are pointed by arrows.

Data information: in (B, D, F–H, J, L), data are presented as mean ± SD. In (B, D, J, L), statistical significance was determined by two-tailed Student's *t*-test. In (F–H), statistical significance was determined by one-way ANOVA with multiple comparisons. Scale bars: 10 μm.

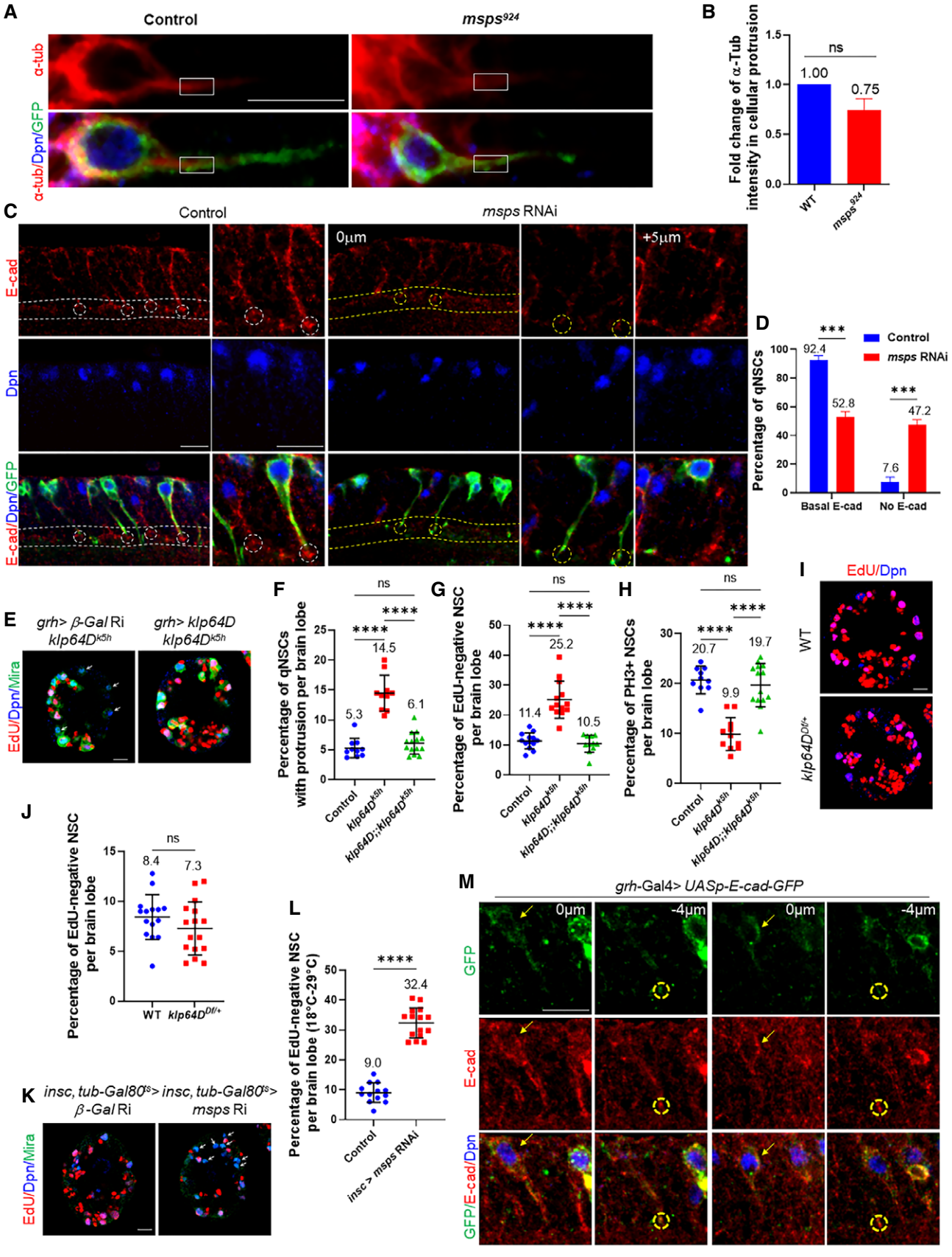

Figure EV4.

Figure EV5. Msps, Kinesin-2, and E-cad function in the same pathway in NSC reactivation.

A Larval brains at 24 h ALH from control (*grh*-Gal4; *UAS-dicer2*/*UAS-β-Gal* RNAi), *kap3* RNAi I (45400), *kap3* RNAi II (103548), *klp64D* RNAi I (BDSC#40945), and *klp64D* RNAi II (103358) expressed under *grh*-Gal4; *UAS-Dicer2* were analyzed for EdU incorporation. Arrows indicate EdU-negative NSCs.

B Quantification graph of EdU-negative NSCs per brain lobe for genotypes in (A). $n = 15$ BL for control; $n = 11$ BL for *kap3* RNAi I; $n = 17$ BL for *kap3* RNAi II; $n = 10$ BL for *klp64D* RNAi I; $n = 11$ BL for *klp64D* RNAi II. ****$P < 0.0001$.

C Quantification graph of the percentage of qNSCs with primary protrusion for genotypes in (A). The protrusion was labeled by Mira. $n = 20$ BL for control; $n = 12$ BL for *kap3* RNAi I; $n = 19$ BL for *kap3* RNAi II; $n = 10$ BL for *klp64D* RNAi I; $n = 13$ BL for *klp64D* RNAi II. ****$P < 0.0001$; ***$P = 0.0004$; **$P = 0.0019$.

D Larval brains at 24 h ALH from RNAi control (*UAS-β-Gal* RNAi; *UAS-β-Gal* RNAi), *msps* RNAi (*UAS-GFP*; *UAS-msps* RNAi (21982)), *kap3* RNAi (*UAS-GFP* + *UAS-kap3* RNAi (103548)), *klp64D* RNAi (*UAS-GFP* + *UAS-Klp64* RNAi (103358)), *msps klp64D* double knockdown (*klp64D* RNAi + *msps* RNAi), and *msps kap3* double knockdown (*kap3* RNAi + *msps* RNAi) driven by *grh*-Gal4 were examined for EdU incorporation, and larval brains were stained with EdU and Dpn. EdU-negative NSCs are indicated by arrows.

E Quantification graph of the percentage of NSCs negative for EdU incorporation per brain lobe for genotypes in (D). $n = 16$ BL for control; $n = 21$ BL for *msps* RNAi; $n = 11$ BL for *kap3* RNAi; $n = 9$ BL for *klp64D* RNAi; $n = 14$ BL for *klp64D* RNAi + *msps* RNAi; $n = 17$ BL for *kap3* RNAi + *msps* RNAi. ****$P < 0.0001$.

F Quantification graph of NSC diameter for genotypes in (D). $n = 192$ NSCs for control; $n = 201$ NSC for *msps* RNAi; $n = 162$ NSCs for *kap3* RNAi; $n = 170$ NSCs for *klp64D* RNAi; $n = 130$ NSCs for *klp64D* RNAi + *msps* RNAi; $n = 247$ NSCs for *kap3* RNAi + *msps* RNAi. ****$P < 0.0001$.

G Larval brains at 24 h ALH from RNAi control (*UAS-β-Gal* RNAi; *UAS-β-Gal* RNAi), *msps* RNAi control (*UAS-GFP*; *UAS-msps* RNAi (21982)), *E-cad* RNAi control (*UAS-GFP* + *UAS-kap3* RNAi (BDSC#38207)), and double knockdown (*E-cad* RNAi + *msps* RNAi) controlled by *grh*-Gal4 were analyzed for EdU incorporation, and larval brains were stained with EdU and Dpn. EdU-negative NSCs are indicated by arrows.

H Quantification graph of the percentage of EdU-negative NSCs per brain lobe for genotypes in (G). $n = 11$ BL for control; $n = 13$ BL for *msps* RNAi; $n = 12$ BL for *E-cad* RNAi; $n = 12$ BL for *E-cad* RNAi + *msps* RNAi. ****$P < 0.0001$; ***$P = 0.0001$.

I Quantification graph of NSC diameter for genotypes in (G). $n = 89$ NSCs for control; $n = 117$ NSCs for *msps* RNAi; $n = 103$ NSCs for *E-cad* RNAi; $n = 216$ NSCs for *E-cad* RNAi + *msps* RNAi. ****$P < 0.0001$.

Data information: in (B, C, E, F, H, I), data are presented as mean ± SD. In (B, C, E, F, H, I), statistical significance was determined by one-way ANOVA with multiple comparisons. Scale bars: 10 μm.

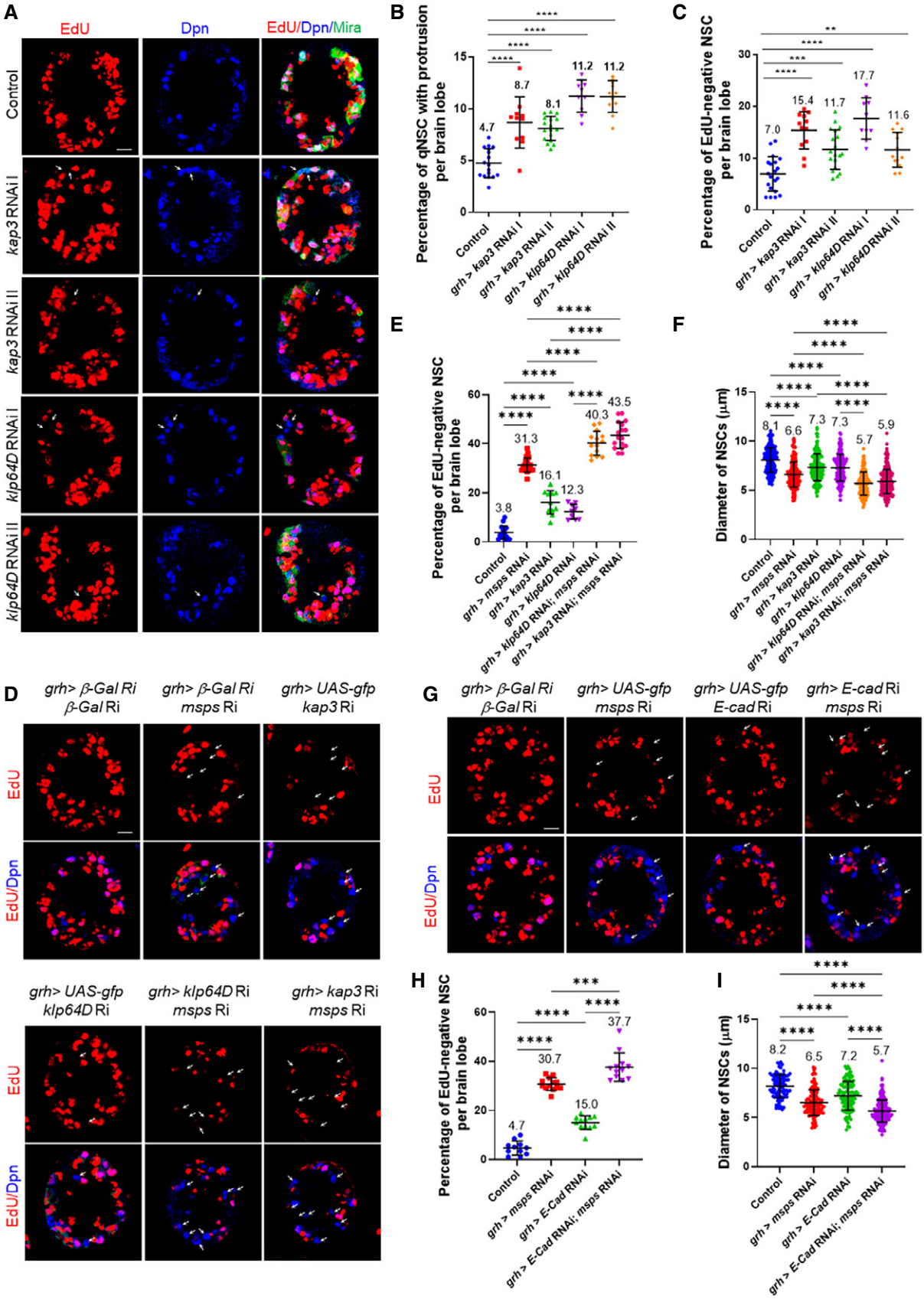

Figure EV5.